Al-Khwarizmi Engineering Journal,Vol. 11, No. 4, P.P. 73- 81 (2015)

Al-Khwarizmi Engineering Journal

Experimental Study and Numerical Simulation of Sheet Hydroforming Process for Aluminum Alloy AA5652

Muthanna Hamza Sadoon* **Sadiq Jaffar Aziz****
Hiba AbdAli Jassim***
*,**,***Department of Mechanical Engineering / University of Technology*
*E-mail: Dr.muthanna@yahoo.com
**E-mail: zaqsam@hotmail.com
***E-mail: hibaabdali@yahoo.com

(Received 31 March 2014 ; accepted 16 June 2015)

Abstract

Lightweight materials is used in the sheet metal hydroforming process, because it can be adapted to the manufacturing of complex structural components into a single body with high structural stiffness. Sheet hydroforming has been successfully developed in industry such as in the manufacturing of the components of automotive.

The aim of this study is to simulate the experimental results (such as the amount of pressure required to hydroforming process, stresses, and strains distribution) with results of finite element analyses (FEA) (ANSYS 11) for aluminum alloy (AA5652) sheets with thickness (1.2mm) before heat treatment (BHT) and after heat treatment (AHT) respectively in the circular die with cavity equals to (20mm) . The comparison of results by these two approaches show the same tendency that an improvement formability, also the plastic deformation is greatly enhanced AHT for same metal.

Keyword : *sheet hydroforming , stress and strain distribution, aluminum alloy, forming limit diagram.*

1. Introduction

Hydroforming is a forming technology for tube and sheet material aiming at high part strength and the manufacturing of complex geometries in one process step. Even straining of the material caused by the fluid pressure leads to a uniform deformation in the sheet, which improves the dent resistance of the hydroforming part compared with conventional stamped parts and the uniform rise in yield strength in the used materials resulting in lower necessary wall thicknesses [1] . Lightweight materials, in particular, aluminum alloys have been widely used in automotive and aircraft industry as the high strength-to-weight ratio of aluminum results in significant weight and fuel savings [2–3]. In addition to weight reduction, utilization of aluminum offers some other advantages such as better corrosion resistance, higher recyclability potential and increased energy absorption during a crash situation.

5XXX alloys, in particular, have the highest formability, and are used in automotive inner panels[4]. Automotive industry has a special interest in AA5754 because of its high ductility, lightweight, strength and weldability properties [5]. However, because of their susceptibility to microstructural damage, aluminum alloy sheets generally exhibits a lower level of formability compared to typical sheet steels [6]. Furthermore, utilization of aluminum alloys in the automotive industry has been far behind of steel because of cost and formability issues at room temperature [7].

In this study, The sheet materials of aluminum (AA5652 t = 1.2mm) was annealed by heavy-duty electric furnace. The annealing temperatures considered for aluminum materials were 345°C. The holding time in the furnace was (1) hour and then cooled in the furnace. The specifications of

furnace include maximum temperature 1000°C, 6.5 kW and 220 V to improve the softer metal and reduce internal stresses in addition to the change in the internal structure of the alloy homogeneity, making it more than it was before the fermentation process.

2. Experimental Procedure

2.1 Chemical Composition

The chemical compositions of sheet material were found out by spectrometry and are reported in Table (1).

Table 1,
Chemical Composition of AA5652.

Material	Element	%Si	%Fe	%Cu	%Mn	%Mg	%Zn	%Cr	%Al
AA5652	Nominal composition	0.4 max.	0.4 max.	0.04 max.	0.01 max.	2.2-2.8	0.1 max.	0.15-0.35	Rem.
	Actual composition	0.095	0.197	0.002	0.013	2.33	0.018	0.280	97

2.2 Uniaxial Tensile Test

The uniaxial tensile test is the basis for defining mechanical properties of materials. It is standardized in ASTM standard E8M specification. The specimens were tested along the three directions, with the tensile axis being parallel (0^o), diagonal (45^o), and perpendicular (90^o) to the rolling direction as showed in figure (1) for specimens with round or rectangular cross sections. Table (2), illustrate the mechanical properties of AA 5652 from tensile test before and after heat treatment respectively .

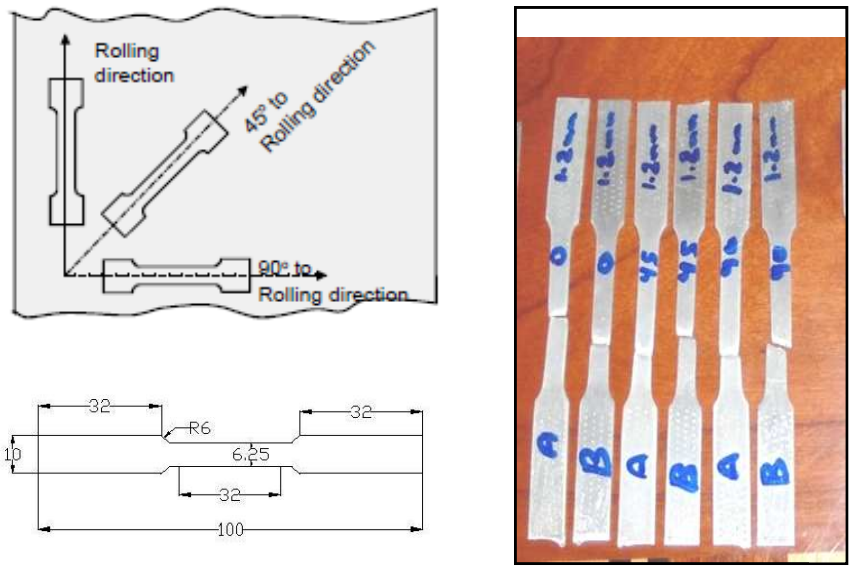

Fig. 1. Tensile specimen BHT and AHT(all dimension in mm).

Table 2,
Shows the mechanical properties of AA 5652 from tensile test before heat treatment.

Material		Young's modulus, E (GPa)	Strain hardening Index n	Hardening coefficient K (MPa)	Anisotropy factor R
AA5652	BHT		0.4	650	0.77
t = 1.2 mm	AHT	70	0.36	575	1

2.3 Hydroforming Sheet

To find out the amount of applied pressure required for the hydroforming process and study the changes in stresses and strain generated in the sheet of aluminum AA5652 (t = 1.2mm) before and after annealing process. Hydroforming die consisting of two parts as show in Figure (2), upper and lower die. The depth of the lower die is (20mm) which was representing die cavity. While the upper die was represent chamber of oil. Blank holder force was 200N to prevent leakage between upper and lower die also to connect the sheet with lower die. Figure (3) shows the specimen shape before and after hydroforming process.

(a) **(b)**

Fig. 2. Hydroforming Die (a) lower die (b)upper die.

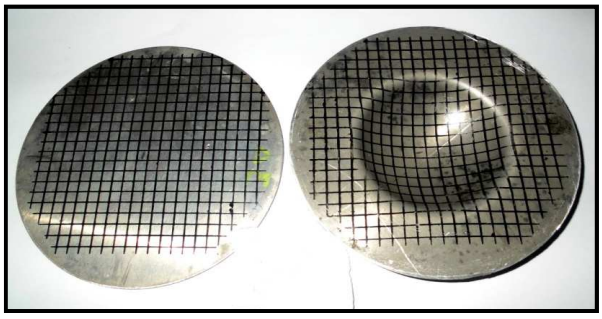

Fig. 3. The specimen before and after hydroforming process.

2.4 Pressure and Depth Measurement

A digital camera type Sony, model DSC-W670, 16.1 Mega pixels was used to record during the hydroforming process. The final results of applied pressure and forming depth can be obtained from the saved movie. In this work, gage pressure device is 600 bars used, the depth during the hydroforming process can be measured by a dial-gauge device. It is attached to the die by an adjective pin of (ϕ $3^{-0.006}$ mm) in diameter which is located in a deep drilled hole in lower half of die to be attached to the lower side of the aluminum sheet, the accuracy of dial-gauge is 0.01mm.

2.5 Forming Limit Diagram

FLD represents the locus of the necked or fractured position of sheet metals in the space of in-plane principal strains, where ε_1 is the major strain and ε_2 is the minor strain. Fld was calculated to AA5652 BHT & AHT as shown in Fingers (4) & (5) to know formability of sheet metal also investigate the maximum strains can be endured without fractured . In order to be able to determine the local deformation of the formed sheet, line patterns with defined geometries (grids) are marked on the sheet specimens prior to forming. The subsequent forming process causes the line patterns to deform by an amount which depends on the local deformation experienced by the sheet part.

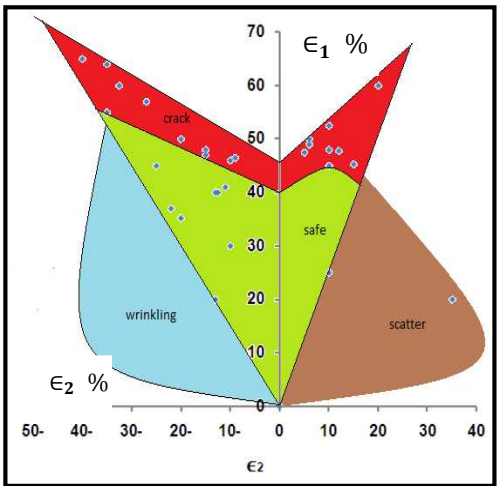

Fig . 4. Forming limit diagram BHT.

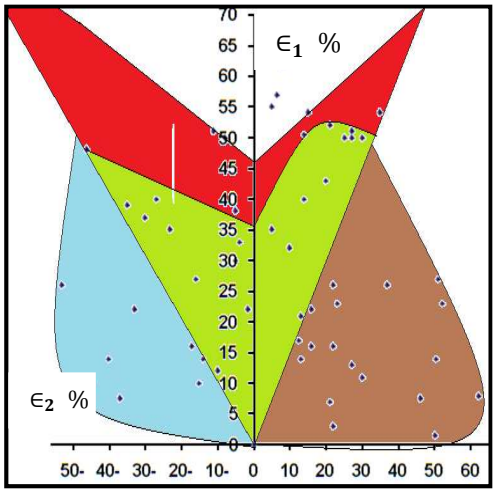

Fig . 5. Forming limit diagram AHT.

3. Finite Element Software Package ANSYS11

ANSYS is a commercial, finite element analysis, software package with capability to analyze a wide range of different problems [8]. For simulating the sheet hydroforming in a circle die processes, commercial FEA software ANSYS11 was used, in which the "Newton-Raphson" implicit approach was employed to solve nonlinear problem. In this approach, the stroke steps on outer surface of blank were defined explicitly over a time span. Within each step, several solutions (substepes or time steps) were performed to apply the pressure gradually. At each substep, a number of equilibrium iterations were performed to obtain a converged solution. Before each solution, the Newton-Raphson method evaluated the out-of-balance load vector, which was the difference between the restoring forces (the loads corresponding to the element stresses) and the applied loads. The 3-D 8-node structural solid element of SOLID95 was used for workpiece (blank).The tool set (die and blank holder) was modeled as rigid bodies. Fluid pressure was defined using a pilot node; this node was also employed to obtain the drawing force during the simulation.

4. Effective Stress & Strain Functions

The work done in deforming the unit element is [9]:

$$\frac{dW}{vol.} = \sigma_1 d\varepsilon_1 + \sigma_2 d\varepsilon_2 + \sigma_3 d\varepsilon_3 \quad \dots (1)$$

For a plane stress process, this becomes [9]:

$$\frac{W}{vol.} = \int_0^{\varepsilon 1} \sigma_1 d\varepsilon_1 + \int_0^{\varepsilon 2} \sigma_2 \, d\varepsilon_2 \quad \dots (2)$$

The plastic work done on a unit volume of material deformed in the tensile test to a true strain of ε_1 (where $\sigma_2 = \sigma 3 = 0$) will be, from Equation (2).

$$\frac{W}{vol.} = \int_0^{\varepsilon 1} \frac{dW}{vol.} = \int_0^{\varepsilon 1} \sigma_1 \, d\varepsilon_1 \quad \dots (3)$$

i.e. the work done per unit volume is equal to the area under the true stress–strain curve. The plastic work done per unit volume in an increment in a process is given by Equation (1). It would useful if this could be expressed in the form

$$\frac{dW}{vol.} = f_1(\sigma_1, \sigma_2, \sigma_3) df_2(\varepsilon_1, \varepsilon_2, \varepsilon_3) \quad \dots (4)$$

As the element is yielding during deformation, a suitable stress function to choose is that given by the von Mises yielding criterion, which has already been shown to have the value of the flow stress. For plane stress this function is: [9]

$$f_1(\sigma_1, \sigma_2, \sigma_3) = \left(\sqrt{1 - \alpha + \alpha^2}\right)\sigma_1 \quad \dots (5)$$

This function is called the representative, effective or equivalent stress, $\overline{\sigma}$, and if the material is yielding, it will be equal to the flow stress. For a general state of stress in an isotropic material the effective stress function is:

$$\bar{\sigma} = \sqrt{\frac{1}{2}\{(\sigma_1 - \sigma_2)^2 + (\sigma_2 - \sigma_3)^2 + (\sigma_3 - \sigma_1)^2\}} \quad \dots (6)$$

In plane stress, the effective stress function is:

$$\bar{\sigma} = \sqrt{\sigma_1^2 - \sigma_1\sigma_2 + \sigma_2^2} = \left(\sqrt{1 - \alpha + \alpha^2}\right)\sigma_1 \quad \dots (7)$$

As indicated, if the material element is at yield, this function will have the magnitude of the flow stress, σ_f. The required strain function in Equation (4) can be found by substitution of the stress function. This function is known as the representative, effective or equivalent strain increment dε and for plane stress, the function is:

$$\overline{d\varepsilon} = df_2(\varepsilon_1, \varepsilon_2, \varepsilon_3) = \sqrt{\frac{4}{3}\{1 + \beta + \beta^2\}} \, d\varepsilon_1 \quad \dots (8)$$

In a general state of stress it can be written as [9]

$$\overline{d\varepsilon} = \sqrt{\frac{2}{3}\{d\varepsilon_1^2 + d\varepsilon_2^2 + d\varepsilon_3^2\}} = \sqrt{\frac{2}{9}\{(d\varepsilon_1 - d\varepsilon_2)^2 + (d\varepsilon_2 - d\varepsilon_3)^2 + (d\varepsilon_3 - d\varepsilon_1)^2\}} \quad \dots (9)$$

In a monotonic, proportional process, Equations (8) and (9) can be written in the integrated form with the natural or true strains ε substituted for the incremental strains dε; i.e. [9]

$$\bar{\varepsilon} = \sqrt{\frac{4}{3}\{1 + \beta + \beta^2\}} \, \varepsilon_1 \quad \dots (10)$$

$$\bar{\varepsilon} = \sqrt{\frac{2}{3}\{\varepsilon_1^2 + \varepsilon_2^2 + \varepsilon_3^2\}} \quad \dots (11)$$

$$\bar{\varepsilon} = \sqrt{\frac{2}{9}\{(\varepsilon_1 - \varepsilon_2)^2 + (\varepsilon_2 - \varepsilon_3)^2 + (\varepsilon_3 - \varepsilon_1)^2\}} \quad \dots (12)$$

where, $\bar{\varepsilon}$, is the representative, effective, or equivalent strain and it can be written in general form as the following[10].

$$\bar{\varepsilon} = \frac{R+1}{\sqrt{2R+1}}\sqrt{1+\frac{2R}{\sqrt{R+1}}\beta+\beta^2} \quad \ldots(13)$$

Where, R represents an average normal anisotropy.

The equation (14) is used to calculate the equivalent stresses [9]

$$\bar{6} = K(\in)^n \quad \ldots(14)$$

5. Results and Discussion

Figure (6) shows the relationship between internal pressure and depth of AA5652 sheet before heat treatment at each load step. In this test the difference between the total internal pressure to form the sheet in both experiments is 4% .The total pressure is 120 bar in experimental test and 125 bar for simulation test**.** The maximum depth was (18 mm) in experimental test and (17.7mm) in simulation test**.**

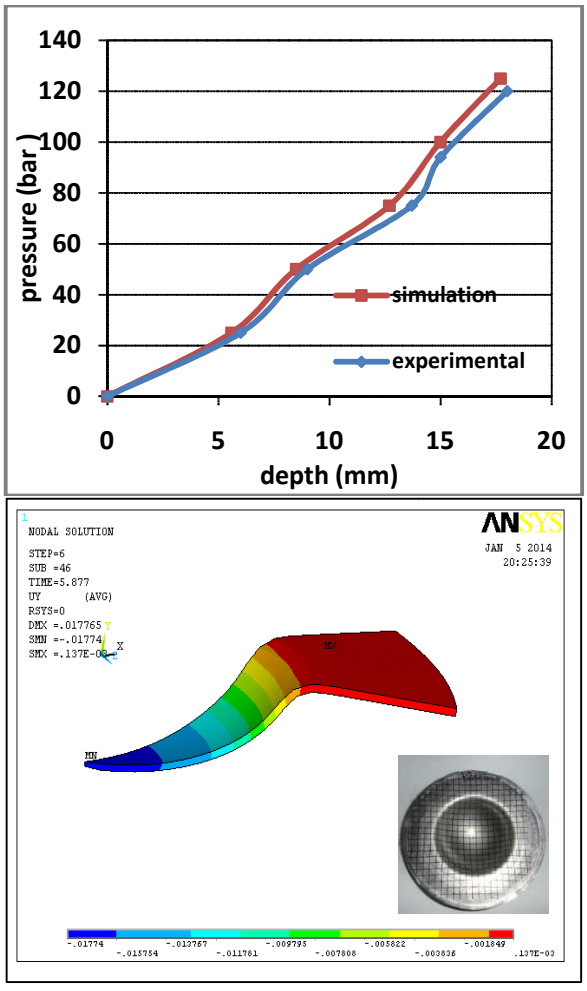

Fig. 6. Relationship between internal pressure and sheet depth (BHT).

While Figure (7) illustrates the maximum depth is (19.8 mm) in experimental test and (19.4 mm) in simulation test of AA5652 sheet after heat treatment under applied pressure equals to that used in before heat treatment. Also, these figures illustrate the effect of heat treatment works cause rearrange the crystals of the metal and increases the formability of the metal for hydroforming which makes the depth of product AHT larger than the depth BHT with same pressure.

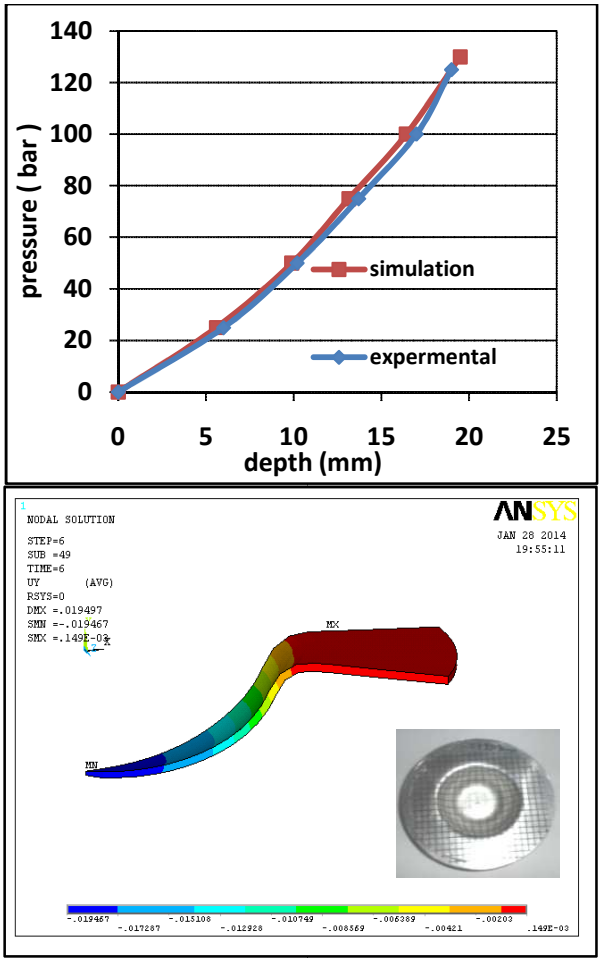

Fig. 7. Relationship between internal pressure and sheet depth (AHT).

Observed approach practical results as Tables (3) and (4) with the results of the simulation program as shown in Figures (8) and (9) for calculating the highest stresses and strains is exposed as a result of the metal hydroforming process before and after heat treatment . Also shows the effect of heat treatment on the behavior of the metal during the hydroforming process, giving more ductility due to re-crystallization of the metal and lower resistance to the stresses to which it is faced.$\in_1, \in_2, \in_3$calculated from the

grids on the cups , also $\bar{\varepsilon}$, $\bar{\sigma}$ calculated by equations (13) and (14) .The observed results are in agreement with the finding of Ref. [11] . The reference used tube hydroforming processes of AA6060 while the current study fouced on sheet hydroforming of AA5652.

Table 3,
Experimental results of the final stage of half AA5652 (t =1.2mm) sheet BHT in a bulge region only.

Pressure	Grid mm	ϵ_1	ϵ_2	ϵ_3	$\bar{\varepsilon}$	$\bar{\sigma}$
	0	0.3987	0.13914	-0.53784	0.5286	503
	5	0.2613	0.09910	-0.3604	0.3521418	428
	10	0.15651	-0.07823	-0.08028	0.156689	310
120 bar	15	0.14188	-0.07323	-0.06865	0.14238	298
	20	0.12321	-0.06823	-0.05498	0.124212	282
	25	0.1159	-0.06011	-0.05579	0.116338	274
	30	0.0965	-0.02356	-0.07294	0.0985923	257

Table 4,
Experimental results of the final stage of half AA5652 (t =1.2mm) sheet AHT in a bulge region only.

Pressure	Grid mm	ϵ_1	ϵ_2	ϵ_3	$\bar{\varepsilon}$	$\bar{\sigma}$
	0	0.5115	0.2201	-0.7316	0.75069	518
	5	0.3286	0.20449	-0.5331	0.53837	460
	10	0.2931	0.1294	-0.4225	0.43289	425.3
120 bar	15	0.2731	-0.1194	-0.1537	0.27381	361
	20	0.253892	-0.083	-0.17089	0.2589	359.72
	25	0.20054	-0.1205	-0.0800	0.20189	323.23
	30	0.17800	-0.096	0.0817 -	0.17820	309

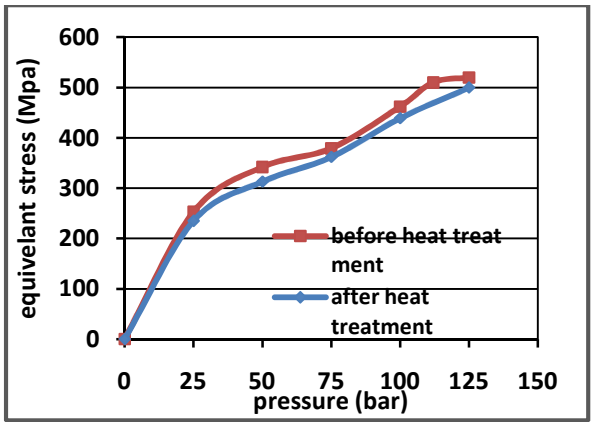

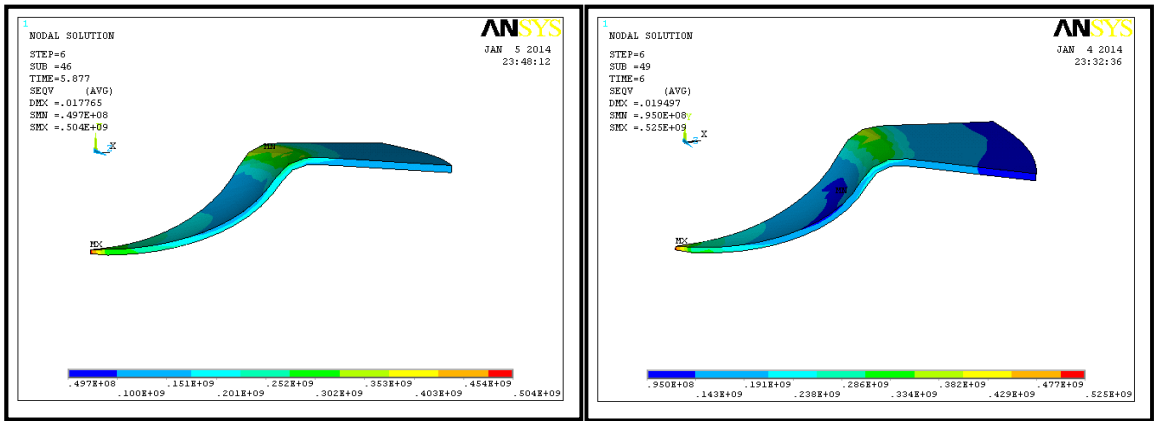

(a) **(b)**

Fig. 8. Relationship between internal pressure and equivalent stress of AA5652 (t =1.2 mm) sheet (a) BHT (b) AHT.

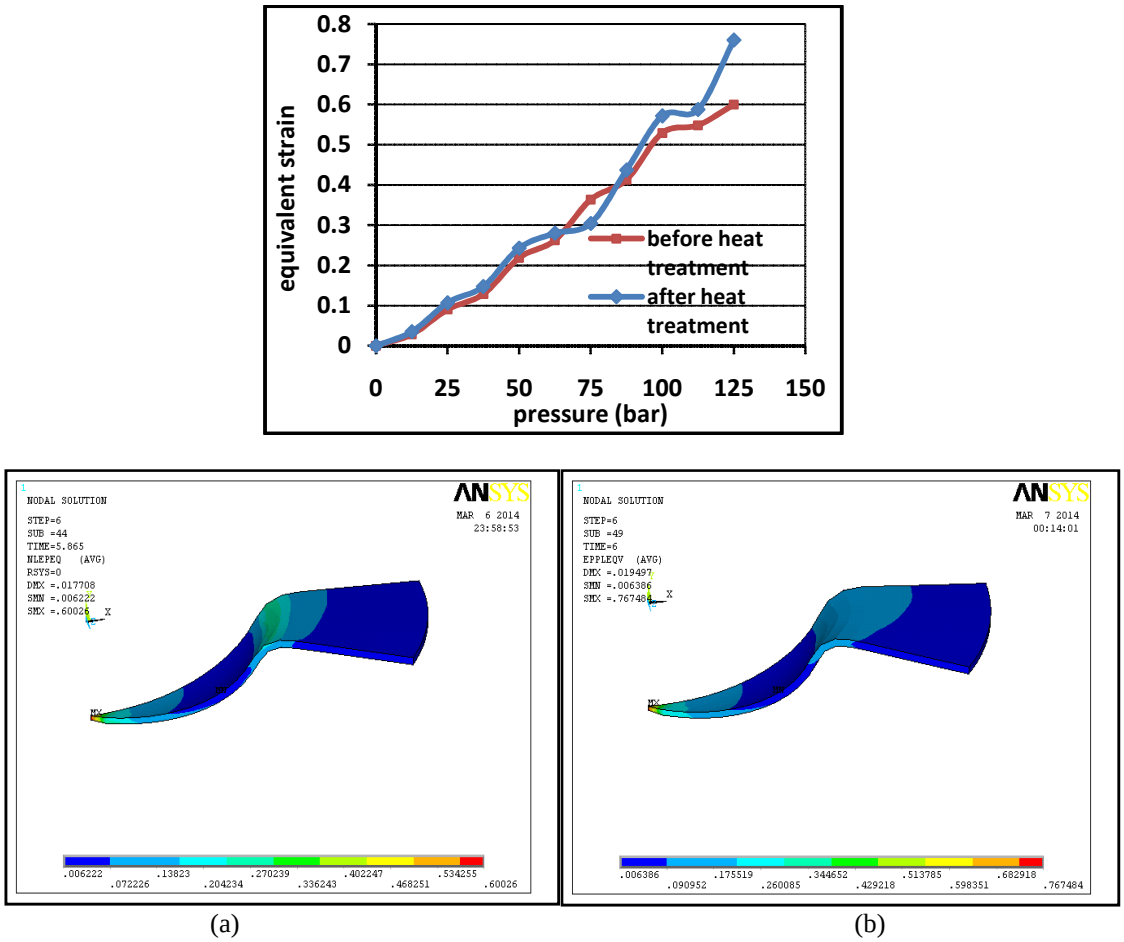

(a) (b)

Fig. 9. Relationship between internal pressure and equivalent strain of AA5652 (t = 1.2 mm) sheet (a) BHT (b) AHT.

6. Conclusions

1. Improving the elongation properties of the metal after heat treatment of the annealing process .
2. Upper value of equivalent stress and equivalent strain BHT were 503 and 0.5286 respectively while AHT become the equivalent stress and equivalent strain 518 MPa and 0.75069 .
3. The hardness increasing after hydroforming process because the work hardening that occur during the process .
4. The pressure required of hydroforming process was lowered AHT, because the characterization of the formability of metal improved .

Notation

$\sigma_1, \sigma_2, \sigma_3$	Principal stresses	(MPa)
$\varepsilon_1, \varepsilon_2, \varepsilon_3$	Principal strains	------
$\bar{\sigma}$	Effective stress	(MPa)
$\bar{\varepsilon}$	Effective strain	------
α	Stress ratio	
β	Strain ratio	
L	Specimen length	mm
w	Specimen length	mm
dl	Change in length	mm
dw	Change in width	mm
dt	Change in thickness	mm

7. References

[1] S. Novotny, M. Geiger, "Process design for hydroforming of lightweight metal sheets at elevated temperatures", Journal of Materials Processing Technology 138, p.p594–599، (2003).

[2] Verbrugge M, Lee T, Krajewski PE, Sachdev A, Bjelkengren C, Roth R, et al. Mass decompounding and vehicle lightweighting. Mater Sci Forum 2009;618– 619:411–8.

[3] Montalbo T, Lee TM, Roth R, Kirchain R. Modeling costs and fuel economy benefits of light weighting vehicle closure Panels. 2008-01-0370, SAE international; 2008.

[4] Bolt PJ, Lamboo NAPM, Rozier PJCM. Feasibility of warm drawing of aluminum products. J Mater Proc Technol 2001;115:118–21.

[5] Wowk DL. Effect of prestrain on the strain rate sensitivity of AA5754 sheet. Ph.D dissertation, Queen's University, Canada; 2008.

[6] Hosford W, Caddell R. Metal Forming. PTR Prentice Hall; 1993.

[7] Ayres RA. Alloying aluminum with magnesium for ductility at warm temperatures (25–250 ºC). Metal Trans A 1979;10:849–54.

[8] ANSYS9.0 manual. SASIP, INC, (2004).

[9] Z.Marciniak, J.L.Duncan, and S.J.Hu, "Mechanics of the sheet metal forming". Second Edition, Butterworth-Heinemann (2002).

[10] V. Gylienė and V. Ostaševičius, " Study of hydroforming by implementing necking criterion in FEM code" , ISSN 1392 - 1207. MECHANIKA. Nr.4(54) ,2005.

[11] SAMI ABBAS HAMMOOD, "Numerical and Experimental Analysis of Tube Hydroforming in a Square Cross-Sectional Die " , M.S .C thesis , University of Technology, Department of Production and Metallurgy Engineering (2012).

الدراسة العملية والعددية لمحاكاة قابلية التشكيل الهيدروليكي لصفائح سبيكة الألمنيوم AA5652

مثنى حمزه سعدون* صادق جعفر عزيز هبه عبد علي جاسم*****

*،**،*** قسم الهندسة الميكانيكية / الجامعة التكنولوجية

*البريد الالكتروني: Dr.muthanna@yahoo.com

** البريد الالكتروني: zaqsam@hotmail.com

*** البريد الالكتروني: hibaabdali@yahoo.com

الخلاصة

استخدمت معادن خفيفة الوزن في عملية تشكيل الصفائح وذلك لتصنيع الهياكل المعقدة بهيئة واحدة وبصلابة عالية . عملية تشكيل الصفائح حققت نجاحا وتطورا في مجال الصناعة كما في تصنيع مكونات السيارات .

ان الهدف من هذه الدراسة هو محاكاة النتائج العملية مثل كمية الضغط المطلوب لعملية التشكيل ، توزيع الاجهادات والانفعالات مع نتائج برنامج التحليل العددي (ANSYS11) لصفائح من سبيكة الالمنيوم AA5652 وبسمك (1.2 mm) قبل وبعد المعاملة الحرارية (التخمير) على التوالي في قالب دائري عمقه (20 mm). مقارنة النتائج العملية مع برنامج المحاكاة كانت متوافقة من حيث تحسين قابلية المعدن على التشكيل وكذلك ازدياد المنطقة اللدنة للمعدن بعد عملية التخمير .